



ELSEVIER

Colloids and Surfaces

A: Physicochemical and Engineering Aspects 167 (2000) 73–81

COLLOIDS
AND
SURFACES

A

www.elsevier.nl/locate/colsurfa

Self-assemblies of block copolymer of 2-perfluorooctylethyl methacrylate and methyl methacrylate

Toyoko Imae ^{a,*}, Hiroyuki Tabuchi ^a, Katsuya Funayama ^a, Ayano Sato ^a,
Tetsuya Nakamura ^b, Naoyuki Amaya ^b

^a *Research Center for Materials Science and Graduate School of Science, Nagoya University, Nagoya 464-8602, Japan*

^b *NOF Corporation, Chita, Aichi 470-2398, Japan*

Abstract

Self-assemblies of poly(methyl methacrylate)-block-poly(2-perfluorooctylethyl methacrylate)-block copolymers in organic solvents were examined. It was confirmed from light scattering that block copolymers formed aggregates of 410 molecules in acetonitrile and of 26 molecules in chloroform. Spherical morphologies were displayed in cryo-transmission electron-microscope (cryo-TEM) photographs and in atomic-force microscope images. The spherical particles consisted of a core of poly(2-perfluorooctylethyl methacrylate) and a shell (corona) of poly(methyl methacrylate). It was elucidated from molecular geometry that the particles in acetonitrile are typical polymer micelles of ≈ 150 Å core radius and ~ 150 Å corona thickness, while those in chloroform are ‘crew-cut’ aggregates. The external contrast variation examination of small-angle neutron scattering and cryo-TEM suggested that the solvent penetration into polymer micelles in acetonitrile is less in the core than in the shell. © 2000 Elsevier Science B.V. All rights reserved.

Keywords: Block copolymer; Poly(2-perfluorooctylethyl methacrylate); Poly(methyl methacrylate); Self-assembly; Polymer micelle; Light scattering; Cryo-transmission electron microscope; Atomic-force microscope; Small-angle neutron scattering; Core-shell model; Crew-cut aggregate

1. Introduction

Colloidal particles often exhibit multidomain structures, which are important in industrial and pharmaceutical applications. Such structures include micelles, microemulsions, and vesicles, which are formed by amphiphilic small molecules

such as surfactants in solutions. Polymer micelles of core-shell (corona) structures have been studied as well as dendrimers, since they have enough large domains for doping chemicals.

Most investigations of amphiphilic copolymers have been for systems containing one hydrophobic block such as styrene [1–6], acrylamide [7], and cinnamoyl ethyl methacrylate [8] and one hydrophilic block like acrylic acid [1,3,4,8], vinylpyridine [2,6], cesium acrylate [5], and ethylene oxide [7]. In other cases, both blocks in

* Corresponding author. Tel.: +81-52-789-5911; fax: +81-52-789-5912.

E-mail address: imae@chem2.chem.nagoya-u.ac.jp (T. Imae)

the copolymers are hydrophobic [9,10] or hydrophilic [11–13], but the tendency is different between blocks. Previous investigations used transmission electron microscopy (TEM) [1–4,6,7,9–11], atomic-force microscopy (AFM) [2], light scattering [1–5,7,9–11], fluorescence spectroscopy [4,8], small-angle neutron scattering (SANS) [5,12], small-angle X-ray scattering [13], potentiometric titration [11], microcalorimetry [11], and electrokinetic analyzer [11] to characterize the copolymers. The copolymers may form micelles of reverse molecular arrangements in aqueous [7,8,11,12] and nonaqueous media [1,2,5,6,9,10] as well as surfactant micelles.

While most of the polymer micelles are spherical [1,2,5–8,10,11], particles of unique structure have also been reported. Ma et al. [4] have revealed a ‘multicore’ micelle structure in mixed solvent. Liu et al. [12] have proposed the ‘cap-and-gown’ model for triblock copolymer micelles. Tao et al. [9] have found that polystyrene-block-poly(2-cinnamoyl ethyl methacrylate) forms star micelles or the mixture of ‘cylindrical’ micelles with stars, depending on the block-length ratio of the copolymer. Yu et al. [3] have presented TEM photographs of ‘crew-cut’ aggregates of block copolymers. The morphology changes from spheres to cylinders, vesicles, tubules, and so on, when the block-length ratio of copolymer, type of solvent, and the solvent ratio in mixed solvent are changed. Alexandridis et al. [13] have reported the nine different phases including micelle phase in a ternary system of block copolymer and selective solvents. The microstructure in each phase has been established.

Novel fluorinated polymers have various commercial uses as coating materials, forming agents, lubricants, and so on, because they exhibit extremely low surface energies. Thomas et al. [14] have reported surface properties of acrylic polymers containing fluorinated monomers. Liu et al. [15] have investigated the morphology of polymer blends including poly(vinylidene fluoride). A rod-like structure of pendant chain perfluorinated ionomer has been confirmed by Loppinet and Gebel [16]. Recently, diblock copolymers of methyl methacrylate and 1H,1H,2H,2H-perfluorooctyl methacrylate (p(MMA-b-F6H2MA))

have been synthesized, and the micellar morphology has been examined by using size-exclusion chromatography, TEM, AFM, and contact angle [17,18].

In the present work, we investigate self-assemblies of block copolymer consisting of 2-perfluorooctylethyl methacrylate (FMA) and methyl methacrylate (MMA). Although both blocks are hydrophobic, Poly(methyl methacrylate) (PMMA) is lipophilic and poly(2-perfluorooctylethyl methacrylate) (PFMA) is lipophobic, indicating the amphiphilicity of PMMA and the amphiphobicity of PFMA. Thus, we can expect that this polymer, poly(methyl methacrylate)-block-poly(2-perfluorooctylethyl methacrylate) (PMMA-b-PFMA, see Fig. 1), forms micelles in nonaqueous media.

2. Experimental section

Anionic block copolymerization of MMA and FMA was carried out as follows; MMA was added in a mixed solution of tetrahydrofuran (THF), LiCl, n-butyl lithium, and diphenylethylene at -78°C under a nitrogen atmosphere. FMA was then added to the resultant PMMA solution in the same conditions. The copolymerization was terminated by adding acidic methanol. The crude solid was recrystallized in methanol, and the purified material was dried in vacuo at 50°C for 24 h. Weight-average molecular weights of PMMA and PMMA-b-PFMA determined by gel-permeation chromatography (GPC) were 41 100 and 78 400, respectively. Their polydispersities were, respectively, 1.03 and 1.07. Then PFMA block has a molecular weight of 37 300. Organic solvents, acetonitrile and chloroform are commercial products.

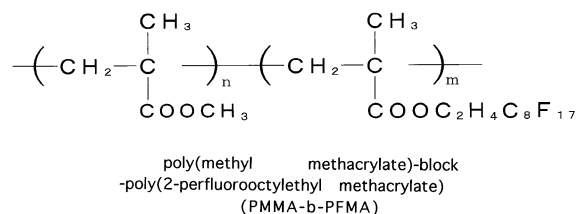


Fig. 1. Chemical structure of PMMA-b-PFMA.

Light scattering was measured at 25°C on an Otsuka Electronics DLS-700 spectrometer. Solutions for light scattering measurements were filtered through a Millipore filter (FH, 0.5 μm). Static light-scattering measurements were performed at angle ranges of 30–150°, and dynamic light scattering was performed at 30, 60, and 90°. The analysis of autocorrelation function on dynamic light scattering was carried out on the basis of an Inverse Laplace Transformation method [19] on an ALV-5000 analyzer equipped on the DLS-700. Details of measurements and analysis are described elsewhere [20–22].

Microscopic observation was carried out at room temperature ($\approx 25^\circ\text{C}$) on a Hitachi H-800 TEM and a DI NanoScope III AFM. A Hitachi H5001-C cold stage was used for cryo-TEM observation. For the preparation of specimens for AFM observations, an aliquot of acetonitrile solution of PMMA-b-PFMA was deposited on a freshly cleaved mica substrate. A chloroform solution was spin-coated on mica. The specimens were then dried. AFM was performed in contact and tapping modes. The microscopy procedures are described elsewhere in more detail [23,24].

SANS measurement was performed at room temperature ($\approx 25^\circ\text{C}$) on a cold neutron instrument WINK at the National Laboratory for High Energy Physics (KEK). A rectangular quartz cell of dimensions 22 \times 40 \times 2 mm was used. 100% D-acetonitrile and mixtures (75, 50, and 25%) of D-acetonitrile and acetonitrile were used as solvents. Details are described elsewhere [25].

3. Results

Fig. 2 illustrates a Zimm plot of static light scattering for acetonitrile solutions of PMMA-b-PFMA at polymer concentrations of 0.90 mg cm^{-3} and less. Weight-average molecular weight M_w , which was calculated from double extrapolation to zero scattering angle and zero polymer concentration, was 31.8×10^6 . Since the value is apparently larger than the molecular weight of monomer (78 400), polymer molecules must aggregate in acetonitrile. Then the aggregation number n_w (aggregate weight/monomer molecular weight)

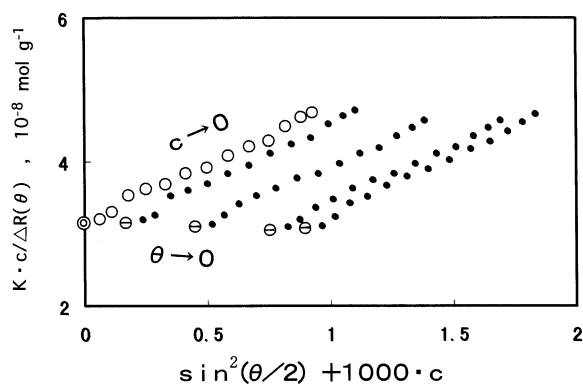


Fig. 2. A Zimm plot of static light scattering for acetonitrile solutions of PMMA-b-PFMA. ●, experimental data; ⊖, extrapolation to zero scattering angle ($\theta \rightarrow 0$); ○, extrapolation to zero polymer concentration ($c \rightarrow 0$); ⊕, double-extrapolation point. K and $\Delta R(\theta)$ are, respectively, the optical constant and reduced scattering intensity difference.

is 410. The radius of gyration of aggregates R_G (359 \AA) was obtained from the extrapolation slope to zero polymer concentration on the Zimm plot. On the other hand, the apparent hydrodynamic radius R_H from dynamic light scattering was evaluated from the diffusion coefficient which was extrapolated to zero scattering angle and zero polymer concentration. The extrapolated value R_H was 306 \AA for aggregates of PMMA-b-PFMA in acetonitrile.

From the Zimm plot for solutions of polymer concentrations of 7.3 mg cm^{-3} and less, the aggregate weight and aggregation number of PMMA-b-PFMA in chloroform were evaluated as 2.26×10^6 and 26, respectively. As compared in Table 1, the aggregation number in chloroform is smaller by one order of magnitude than that in acetonitrile. A much smaller aggregation number was obtained in THF. On the elution process in a GPC column, in the early stages before the monomer was eluted, there was a peak that indicated the presence of aggregated species. The estimated molecular weight was 0.648×10^6 , which corresponds to an aggregation number of 8.3. The characteristic numerical values are listed in Table 1 with those of the related parameters, the refractive index of solvent n_0 and the specific refractive index increment $\partial_n/\partial c$.

Table 1
Characteristics of polymer micelles of PMMA-b-PFMA in organic solvents

Solvent	n_0	∂_n/∂_c (cm ³ g ⁻¹)	M_w ($\times 10^{-6}$)	n_w	R_G (Å)	R_H (Å)	R_{TEM} (Å)	R_{AFM} (Å)
Acetonitrile	1.345	0.073	31.8	410	359	306	100–200	250–350
Chloroform	1.447	0.00849	2.26	26			150–250	

A cryo-TEM photograph of an acetonitrile solution of PMMA-b-PFMA at 0.90 mg cm⁻³ is shown in Fig. 3. Nearly spherical particles with radii R_{TEM} of 100–200 Å were observed. Fig. 4 gives AFM images for specimen prepared from acetonitrile and chloroform solutions of PMMA-b-PFMA at 1 mg cm⁻³. It was elucidated from the images that the spherical particles accumulated on mica substrates. The estimated radii R_{AFM} were 250–350 Å for acetonitrile solution and 150–250 Å for chloroform solution. Spherical images of similar size were observed even for the chloroform solution of 107 mg cm⁻³. It should be noticed that the R_{TEM} of polymer aggregates in acetonitrile is smaller than that the R_H and R_{AFM} . Moreover, R_{AFM} values of aggregates in chloroform are smaller than values measured in acetonitrile. The numerical values are included in Table 1.

SANS was measured for solutions of PMMA-b-PFMA at 3 mg cm⁻³ in 100% D-acetonitrile and mixtures of D-acetonitrile and acetonitrile (75, 50, and 25% D-acetonitrile). Fig. 5 illustrates scattering intensities $I(Q)$ as a function of scattering vector Q for solutions of 100 and 50% D-acetonitrile. On the Guinier plot, the intensities decreased almost parallel with decreasing D-acetonitrile content, indicating less significant size changes, although the neutron-scattering-length density of solvent decreased.

4. Discussion

Light scattering measurements and microscopic observations support the formation of spherical polymer micelles of PMMA-b-PFMA in acetonitrile and chloroform solutions. Micellar size in acetonitrile is larger than that in chloroform, indicating a solvent dependence on micelle formation.

The morphogenic effect of solvent on aggregates has been reported for polystyrene-b-poly(acrylic acid) diblock copolymers by Yu et al. [3]. They found that lower polarity solvents cause weaker poly(acrylic acid)-solvent interactions and therefore result in weaker repulsive interactions in the corona. This phenomena increases the aggregation number. Since the dielectric constants are in the order of acetonitrile < chloroform < THF, the interpretation of aggregation reinforcement depending on polarity is also applicable for the present system of PMMA-b-PFMA.

PFMA block is lipophobic, but PMMA block is conversely lipophilic. Then, while PFMA blocks aggregate to form a micelle core, PMMA blocks construct a shell and expand like a corona over the core, because PMMA chains take on a ran-

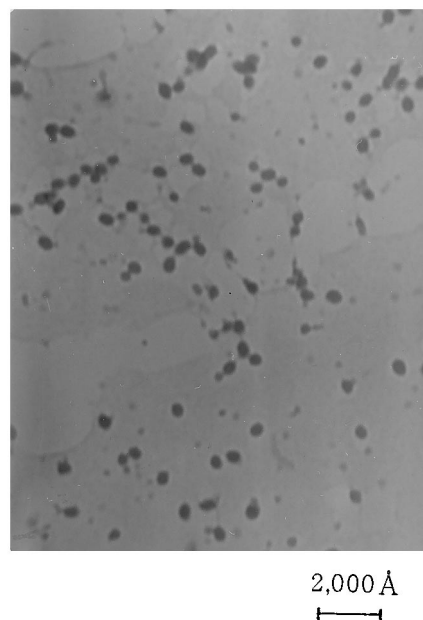


Fig. 3. A cryo-TEM photograph of an acetonitrile solution of PMMA-b-PFMA at 0.90 mg cm⁻³.

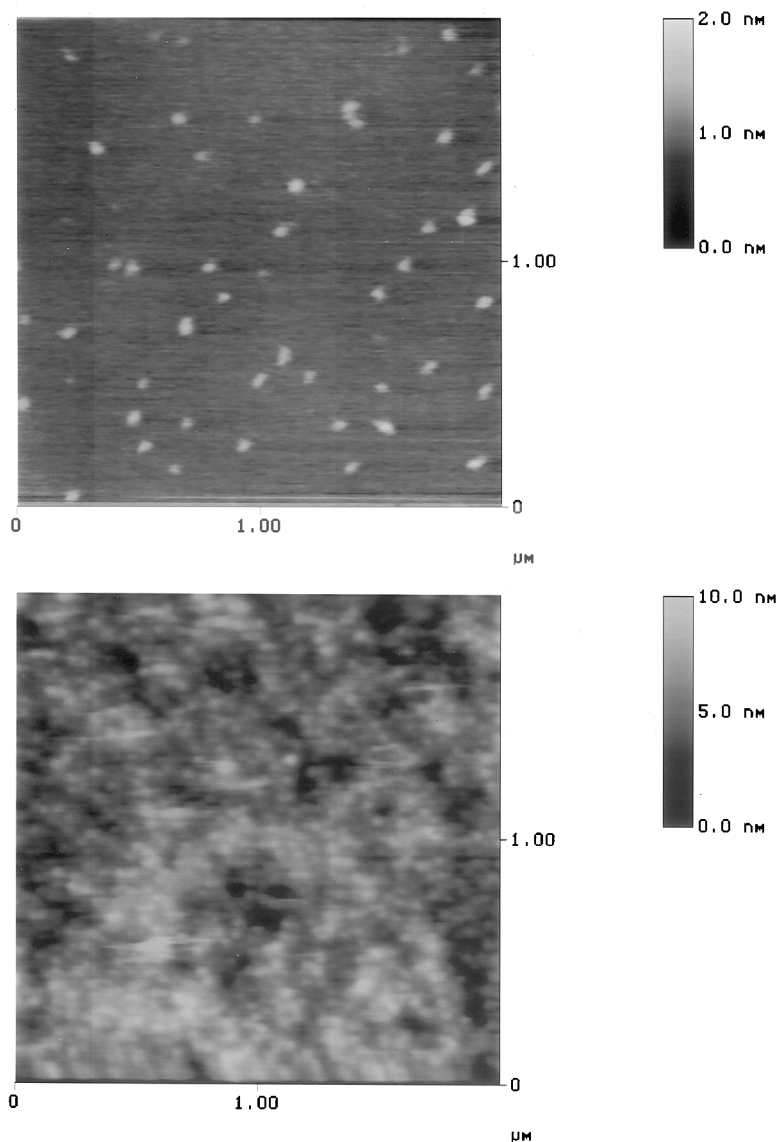


Fig. 4. AFM images for specimen prepared from acetonitrile (upper) and chloroform (lower) solutions of PMMA-b-PFMA at 1 mg cm^{-3} .

domly coiled structure and have affinities for acetonitrile and chloroform. PFMA block consists of a perfluorooctylethyl $\text{CF}_3(\text{CF}_2)_7\text{C}_2\text{H}_5$ side chain, the perfluorooctyl part of which is rather like rigid rods, and the back-bone chain of which takes on a trans-zigzag configuration.[26] Then, the cross-sectional diameter of the side chain is 6.2 \AA , since C–C distance, C–F distance, and the radius of F

in the cross-section are 3.1, 1.34, and 1.47 \AA , respectively. PFMA block consists of 70.1 units of FMA (aggregate weight of PFMA/unit weight of FMA = $37\,300/532.2$). As the first approximation, a trans-zigzag backbone-chain configuration can be supposed for the PFMA chain structure. However, this model is impossible because of the steric hindrance between fluorocarbon side chains (see

Fig. 6). That is, the calculated distance between perfluorooctyl side chains is only 2.51 Å ($2 \times \text{C-C distance} \times \sin(\text{C-C-C-angle}/2) = 2 \times 1.54 \sin(109.5^\circ/2)$ Å), while the cross-sectional diameter of the side chain is 6.2 Å.

Instead, a trans-gauche type configuration, which is known as a structure of isotactic polypropylene in crystal, is proposed as a structural model of the PFMA chain. Then the perfluorooctyl side chains are not hindered spatially with each other but arrange radially, as illustrated in Fig. 5, because the distance ($6.5 \text{ Å} = 2.17 \text{ Å per}$

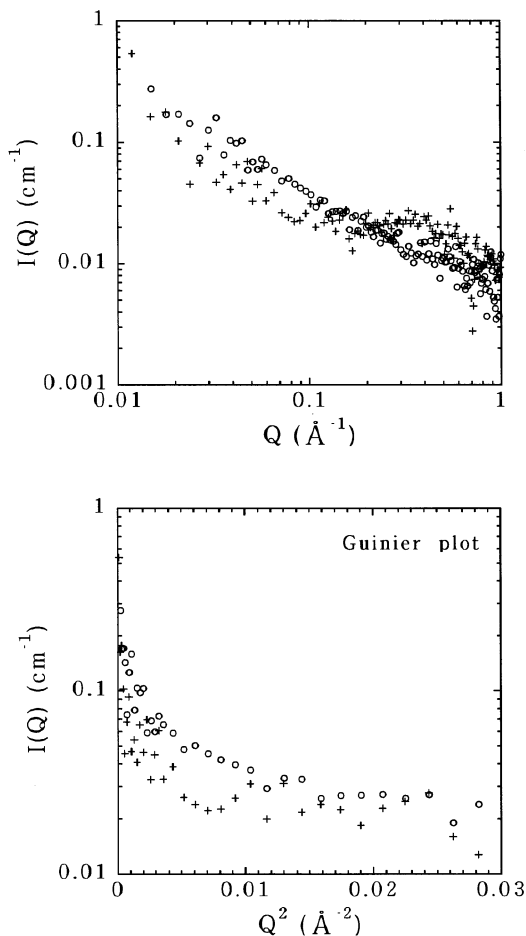


Fig. 5. SANS intensities $I(Q)$ as a function of scattering vector Q for solutions of PMMA-*b*-PFMA at 3 mg cm^{-3} in 100% D-acetonitrile (○) and equimolar mixture of D-acetonitrile and acetonitrile (x). Upper, double logarithmic plot; lower, Guinier plot.

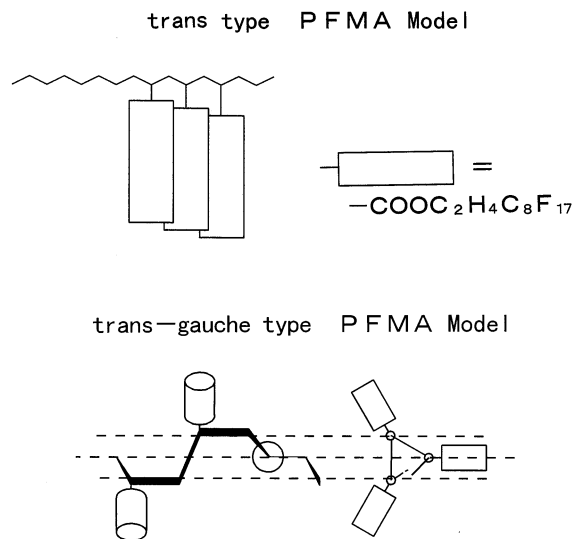


Fig. 6. The schematic illustration of trans type and trans-gauche type PFMA model.

pitch $\times 3$) between side chains is wider than the diameter of the side chains. In this model, the distance from the center axis of the PFMA chain to the terminal end of the perfluorooctyl side chain is 16.9 Å ($(2 + 1.34n_F + 1.265n_H + 3.4/2)$ Å, $n_F = 7$; $n_H = 3$), and the length of the PFMA chain is 152 Å ($2.17 \text{ Å} \times 70.1$), because one pitch length is 2.17 Å. Other chain configurations such as trans-trans-gauche or trans-gauche-gauche type are also supported, and then the lengths of PFMA may be shorter than that of PFMA with the trans-gauche configuration.

When the core radius of amphiphobic PFMA block in acetonitrile is 152 Å, the shell thickness of the PMMA block must be 154 Å, because the hydrodynamic radius obtained from dynamic light scattering is 306 Å. A schematic representation of a trans-gauche PFMA chain structure and polymer micelle structure in acetonitrile is illustrated in Fig. 7. Since the molecular weight of PMMA is 41 100, the degree of polymerization is calculated as 411 from a monomer molecular weight of 100.1. If the PMMA chain takes on a trans-zigzag configuration, the chain length is 1030 Å ($2.51 \text{ Å} \times 411$). On the other hand, if the chain is a freely jointed random coil, the end-to-end distance is 50.9 Å ($411^{1/2} \times 2.51 \text{ Å}$). Then the

possible length range of the PMMA chain is 50–1030 Å. The corona thickness of the PMMA chain estimated above is within the possible size.

While the micelle size in the AFM image from acetonitrile solution of PMMA-*b*-PFMA is consistent with that from dynamic light scattering, the size in cryo-TEM is smaller than those in AFM and in light scattering and rather equivalent to the PFMA core size. This is concerned in the fact that different techniques gave different sizes. The corona with penetrated solvent is distinguished from the core but not from solvent under the electron beam on cryo-TEM photographs. In other words, it is considered that, during the electron-beam irradiation on cryo-TEM measurement, the electron transmission of the electron-dense PFMA core is different from that of electron-less PMMA corona which has a similar electron density to bulk solvent. Therefore, one can detect only the core size in cryo-TEM.

The experimental data for polymer micelles in chloroform is too little to determine the exact structure. Although the aggregation number in

chloroform is smaller by 1/16 times than that in acetonitrile, the ratio of micelle diameter in chloroform and acetonitrile is only 2/3. The proposed micelle structure in chloroform is compared with that in acetonitrile, as illustrated in Fig. 8. Although micelles in chloroform consist of smaller numbers of molecules, they may have cores of radii 150 Å, because PFMA blocks have a rigid rod structure. PMMA blocks may extend on the core outside and construct a thin shell, because the core surface area per molecule is large. This type of structure is called ‘crew-cut’ [3]. Another possible micelle structure in chloroform is one in which the PFMA blocks are bent and packed in the core. However, facts supporting this model were not obtained.

As estimated from aggregation numbers and the proposed structure illustrated in Fig. 8, because micelles in acetonitrile are compact, it can be assumed that solvent molecules penetrate poorly into the micelle core at least. This was elucidated from the fact that, in the external contrast variation examination, SANS curves

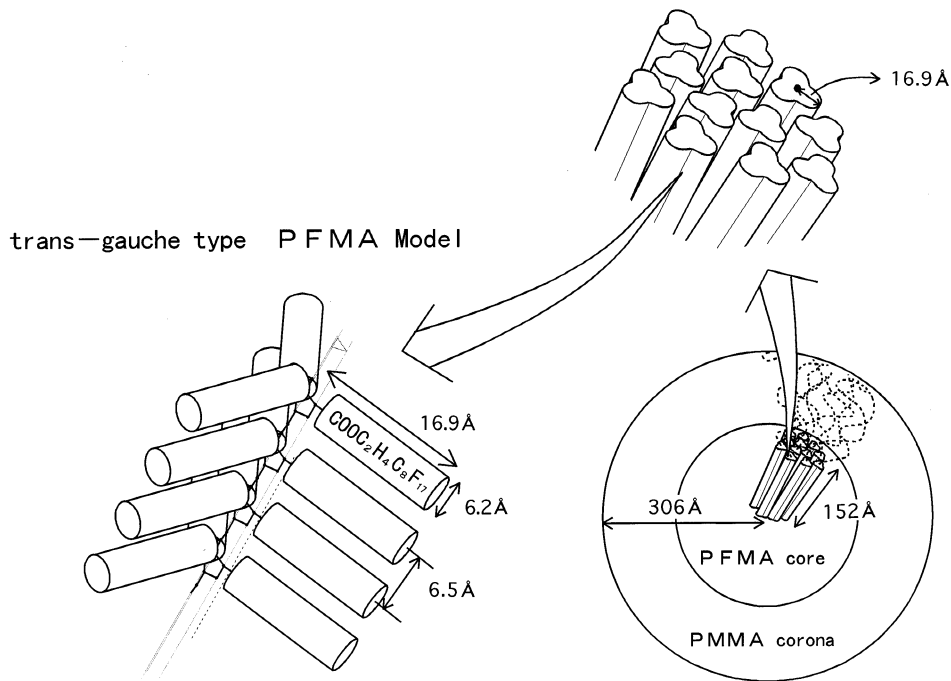


Fig. 7. The schematic representation of trans-gauche PFMA chain structure and polymer micelle structure in acetonitrile.

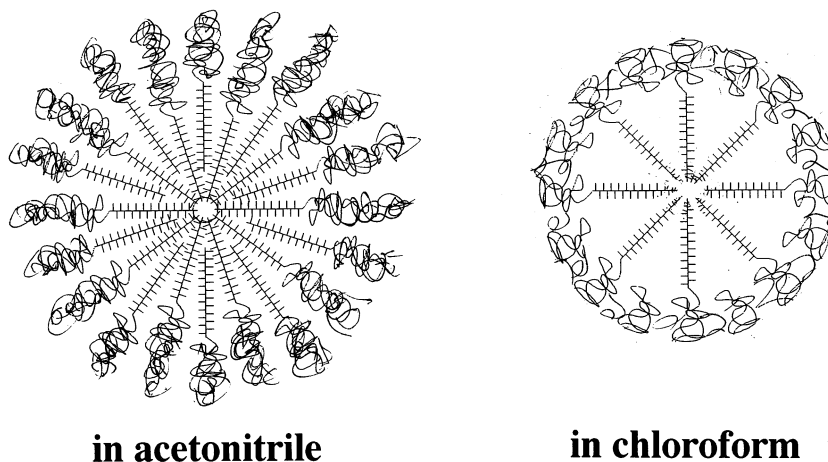


Fig. 8. Illustration of proposed structures for polymer micelles in acetonitrile and chloroform.

were not changed. This character of polymer micelles is completely different from dendrimers. It has been confirmed that amido amine dendrimers can dope water molecules in their interiors [27]. The incorporation of small molecules in polymer micelles has been reported by Wang et al. [8]. Poly(2-cinnamoyl ethyl methacrylate)-block-poly(acrylic acid) nanospheres take perylene in the core. This is not the case with PMMA-*b*-PFMA micelles, because their cores consist of amphiphobic perfluorinated blocks.

Krupers et al. [18] have reported that diblock copolymers of methyl methacrylate and 1H, 1H,2H,2H-perfluorooctyl methacrylate (p(MMA-*b*-F6H2MA)) form cylindrical micelles in THF. The difference between their results and those in the present paper should be noted, because the chemical structure of p(MMA-*b*-F6H2MA) is very similar to that of PMMA-*b*-PFMA. Tao et al. [9] have inferred that polystyrene-block-poly(2-cinnamoyl ethyl methacrylate) (PS-*b*-PCEMA) molecules form star micelles, if the number ratio of styrene units to PCEMA units, that is, unit number in shell:unit number in core, is greater than 9. On the other hand, at number ratios between 7 and 8.2, cylindrical micelles coexist with star micelles. The unit number in shell unit number in core value ($5.9 = 411/70.1$) for PMMA-*b*-PFMA in the present work must be larger than the corresponding value for p(MMA-*b*-

F6H2MA), since spherical PMMA-*b*-PFMA micelles are formed in acetonitrile and chloroform.

5. Conclusions

Self-assemblies of block copolymers of methyl methacrylate and 2-perfluorooctylethyl methacrylate (PMMA-*b*-PFMA) were investigated in organic solvents. It was confirmed from light scattering that block copolymers formed aggregates of 410 molecules with a 306 Å radius in acetonitrile. A cryo-TEM photograph and AFM image displayed a spherical morphology. It was concluded from the geometric considerations of polymer molecules that the spherical particles were polymer micelles with a PFMA core of a 152 Å radius and a PMMA corona (shell) of 154 Å thickness.

On an external contrast-variation examination of SANS measurement for polymer micelles, Guinier plots decreased at a similar tendency when the D-acetonitrile/acetonitrile fraction was changed. It was suggested that the polymer micelles of PMMA-*b*-PFMA behaved as hard spheres in which acetonitrile molecules penetrated poorly.

Polymer micelles in chloroform consisted of 26 molecules, and the radius was smaller than that in

acetonitrile. This means that the aggregation number of polymer micelles depends on the solvent. Moreover, PMMA blocks may extend on the core surface in chloroform, while PMMA blocks extend far away from the core surface in acetonitrile.

References

- [1] L. Zhang, H. Shen, A. Eisenberg, *Macromolecules* 30 (1997) 1001.
- [2] J.C. Meiners, A. Quintel-Ritzi, J. Mlynek, H. Elbs, G. Krausch, *Macromolecules* 30 (1997) 4945.
- [3] Y. Yu, L. Zhang, A. Eisenberg, *Macromolecules* 31 (1998) 1144.
- [4] Y. Ma, T. Cao, S.E. Webber, *Macromolecules* 31 (1998) 1773.
- [5] M. Moffitt, Y. Yu, D. Nguyen, V. Graziano, D.K. Schneider, A. Eisenberg, *Macromolecules* 31 (1998) 2197.
- [6] F.J. Esselink, E. Dormidontova, G. Hadziioannou, *Macromolecules* 31 (1998) 2925.
- [7] M.D.C. Topp, P.J. Dijkstra, H. Talsma, J. Feijen, *Macromolecules* 30 (1997) 8518.
- [8] G. Wang, F. Henselwood, G. Liu, *Langmuir* 14 (1998) 1554.
- [9] J. Tao, S. Stewart, G. Liu, M. Yang, *Macromolecules* 30 (1997) 2738.
- [10] J. Tao, G. Liu, J. Ding, M. Yang, *Macromolecules* 30 (1997) 4084.
- [11] T.K. Bronich, A.V. Kabanov, V.A. Kabanov, K. Yu, A. Eisenberg, *Macromolecules* 30 (1997) 3519.
- [12] Y. Liu, S.-H. Chen, J.S. Huang, *Macromolecules* 31 (1998) 2236.
- [13] P. Alexandridis, U. Olsson, B. Lindman, *Langmuir* 14 (1998) 2627.
- [14] R.R. Thomas, D.R. Anton, W.F. Graham, et al., *Macromolecules* 30 (1997) 2883.
- [15] L.-Z. Liu, B. Chu, J.P. Penning, R.S.J. Manley, *Macromolecules* 30 (1997) 4398.
- [16] B. Loppinet, G. Gebel, *Langmuir* 14 (1998) 1977.
- [17] M.J. Krupers, M. Möller, *Macromol. Chem. Phys.* 198 (1997) 2163.
- [18] M.J. Krupers, S.S. Sheiko, M. Möller, *Polymer Bulletin* 40 (1998) 211.
- [19] N. Ostrowsky, D. Sornette, P. Parker, E.R. Pike, *Exponential sampling technique*, *Optica Acta* 28 (1981) 1059.
- [20] T. Imae, S. Ikeda, *Colloid Polym. Sci.* 265 (1987) 1090.
- [21] T. Imae, *J. Phys. Chem.* 92 (1988) 5721.
- [22] T. Imae, *J. Colloid Interface Sci.* 127 (1989) 256.
- [23] T. Imae, Y. Takahashi, H. Muramatsu, *J. Am. Chem. Soc.* 114 (1992) 3414.
- [24] O. Mori, T. Imae, *Langmuir* 11 (1995) 4779.
- [25] T. Imae, M. Kakitani, M. Kato, M. Furusaka, *J. Phys. Chem.* 100 (1996) 20051.
- [26] D. Jacquemain, S.G. Wolf, F. Leveiller, et al., *J. Am. Chem. Soc.* 112 (1990) 7724.
- [27] T. Imae, K. Funayama, K. Aoi, K. Tsutsumiuchi, M. Okada, M. Furusaka, *Langmuir* 15 (1999) 4076.